Controlled Fabrication of Hollow Metal Pillar Arrays Using Colloidal Masks

ARTICLE *in* CHEMISTRY OF MATERIALS · NOVEMBER 2006

Impact Factor: 8.35 · DOI: 10.1021/cm060731j

4 AUTHORS, INCLUDING:

Se Gyu Jang
Korea Institute of Science and Technology
54 PUBLICATIONS **1,506** CITATIONS
SEE PROFILE

Dae-Geun Choi
Korea Institute of Machinery and Materials
106 PUBLICATIONS **1,821** CITATIONS
SEE PROFILE

Controlled Fabrication of Hollow Metal Pillar Arrays Using Colloidal Masks

Se Gyu Jang,† Hyung Kyun Yu,† Dae-Geun Choi,‡ and Seung-Man Yang*,†

National Center for Integrated Optofluidic Systems and Department of Chemical and Biomolecular Engineering, Korea Advanced Institute of Science and Technology, Daejeon 305-701, Korea, and Nano-Mechanical Systems Research Center, Korea Institute of Machinery & Materials, 171 Jang-dong, Yuseong-gu, Daejeon 305-343, Korea

Received March 28, 2006
Revised Manuscript Received September 9, 2006

Colloidal lithography (CL) is an emerging technique for 2D nanopatterns.[1] The promising advantage of CL over advanced lithographic techniques is the simple and fast creation of large area nanopatterns through the self-organization of colloids. A variety of types of unit patterns ranging from dots to polygonal have been fabricated with CL for diverse applications.[2] Nevertheless, the fabrication of nanotubes and their 2D arrays with CL remains challenging because of the lack of the controllability and the low aspect ratio of the resulting structure. Furthermore, most of the previous studies using the dry etching over a colloidal mask have produced dome-shaped structures rather than the straight pillars. These unsolved issues arise mainly from the under-etching of the substrate around the contact point with colloidal mask and the simultaneous etching of both the mask and the substrate.[3] Although a seeded growth of nanotubes or an additional metallic mask has been employed for enhancement of the etching contrast,[4] these methods are limited by the material availability and are not suitable for the fabrication of hollow structures.

Here, we report a novel approach for fabricating a 2D hollow nanopillar array using reactive ion etching (RIE) through inorganic nanosphere arrays over a polymeric film for higher etching contrast. Our strategy offers reproducibility on diverse substrates, simplicity of process, and feasibility for morphological control of nanopillar arrays. Hollow nanopillar arrays of gold and molybdenum were created directly on substrates over large areas without a pattern transfer process, frequently employed in the fabrication of nanotubes using porous template.[5] The geometric features of the nanopillars were controlled by simply adjusting the polymer film thickness and the RIE and metal-sputtering conditions. Furthermore, the aforementioned under-etching of the substrate could be avoided by depositing an additional polymeric layer, which eventually yielded an ordered array of straight hollow nanopillars. As an illustrative application, the Molybdeum (Mo) hollow nanopillar array fabricated here showed a low turn-on voltage and can be applied for field-emission-related devices. Also, the flexibility in controlling the nanotube morphology is of practical significance in optics and biotechnology.

Scheme 1. Fabrication Scheme of Hollow Nanopillar Array

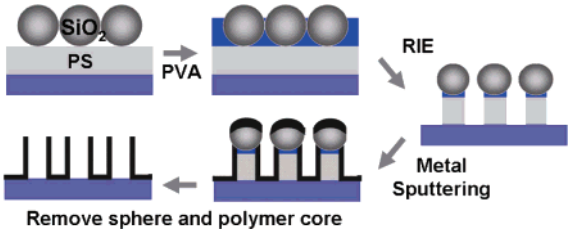

Scheme 1 illustrates our strategy for fabricating a hollow metal nanopillar array. Hexagonally ordered silica spheres were self-organized by spin-casting of a silica colloid on a spin-cast polystyrene (PS) film on diverse substrates, namely, silicon wafer, sputtered gold, indium tin oxide (ITO), and glass. The thickness of the PS film was controlled by adjusting both the concentration of the PS solution and the spin speed. To facilitate the spin-casting of both hydrophilic silica dispersion and aqueous poyl(vinylalcohol) (PVA) solutions on a hydrophobic PS surface, we exposed the PS film to mild O_2 plasma.[6] The contact angle between the water−air interface and the O_2 plasma-treated PS film was less than 10°, indicating that the PS surface became hydrophilic. Silica dispersion in ethanol was spun-cast for the monolayer of silica array. The average crystal domain sizes of silica monolayers were about 750 and 520 μm^2 in the cases of 530 and 320 nm arrays of silica spheres, respectively. Vacant space under the silica spheres over the PS film was filled with PVA by spin-casting an aqueous PVA solution. A mixture of CF_4 and O_2 RIE for opening windows between the silica spheres and O_2 RIE for the creation of the PS nanocylinder array was conducted sequentially. The O_2 RIE proceeded until the rough polymeric layer was removed completely, and the appropriate RIE time was

* Corresponding author. E-mail: smyang@kaist.ac.kr.
† Korea Advanced Institute of Science and Technology.
‡ Korea Institute of Machinery & Materials.

(1) (a) Hulteen, J. C.; van Duyne, R. P. *J. Vac. Sci. Technol., A* **1995**, *13*, 1553. (b) Choi, D.-G.; Yu, H. K.; Jang, S. G.; Yang, S.-M. *J. Am. Chem. Soc.* **2004**, *126*, 7019. (c) Choi, D.-G.; Kim, S.; Lee, E.; Yang, S.-M. *J. Am. Chem. Soc.* **2005**, *127*, 1636. (d) Kosiorek, A.; Kandulski, W.; Glaczynska, H.; Giersig, M. *Small* **2005**, *1*, 439.
(2) (a) Haes, A. J.; william, L. C.; Klein, L.; van Duyne, R. P. *J. Am. Chem. Soc.* **2005**, *127*, 2264. (b) Lu, Y.; Liu, G. L.; Kim, J.; Mejia, Y. X.; Lee, L. P. *Nano. Lett.* **2005**, *5*, 119. (c) Albrecht, M.; Hu, G.; Guhr, I. L.; Ulbrich, T. C.; Boneberg, J.; Leiderer, P.; Schatz, G. *Nat. Mater.* **2005**, *3*, 203. (d) Wang, C.; Zhang, Y. *Adv. Mater.* **2005**, *17*, 150.
(3) (a) Tan, B. J.-Y.; Sow, C.-H.; Lim, K.-Y.; Cheong, F.-C.; Chong, G.-L.; Wee, A. T.-S.; Ong, C.-K. *J. Phys. Chem. B* **2004**, *108*, 18575. (b) Aizpurua, J.; Hanarp, P.; Sutherland, D. S.; Kall, M.; Bryant, G. W.; de Abajo, F. G. J. *Phys. Rev. Lett.* **2003**, *90*, 057401. (c) Valsesia, A.; Colpo, P.; Silvan, M. M.; Meziani, T.; Ceccone, G.; Rossi, F. *Nano. Lett.* **2004**, *4*, 1047.
(4) (a) Kempa, K.; Kimball, B.; Rybczynski, J.; Huang, Z. P.; Wu, P. F.; Steeves, D.; Sennett, M.; Giersig, M.; Rao, D. V. G. L. N.; Carnahan, D. L.; Wang, D. Z.; Lao, J. Y.; Li, W. Z.; Ren, Z. F. *Nano. Lett.* **2003**, *3*, 13. (b) Wang, X.; Summers, C. J.; Wang, Z. L. *Nano. Lett.* **2004**, *4*, 423. (c) Kuo, C.-W.; Shiu, J.-Y.; Chen, P. *Chem. Mater.* **2003**, *15*, 2917.
(5) (a) Qu, L.; Shi, G.; Wu, X.; Fan, B. *Adv. Mater.* **2004**, *16*, 1200. (b) Lee, W.; Alexe, M.; Nielsch, K.; Gosele, U. *Chem. Mater.* **2005**, *17*, 3325. (c) Mu, C.; Yu, Y.; Wang, R.; Wu, K.; Xu, D.; Guo, G. *Adv. Mater.* **2004**, *16*, 1550. (d) Son, S. J.; Reichel, J.; He, B.; Schuchman, M.; Lee, S. B. *J. Am. Chem. Soc.* **2005**, *127*, 7316.
(6) Guruvenket, S.; Rao, M. G.; Komath, M.; Raichur, A. M. *Appl. Surf. Sci.* **2004**, *236*, 278.

10.1021/cm060731j CCC: $33.50
Published on Web 11/30/2006

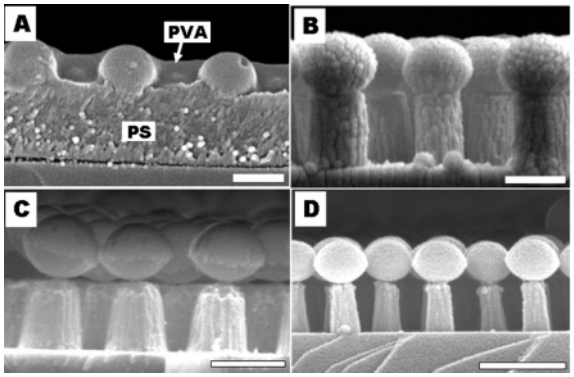

Figure 1. (a) SEM cross-section image of PVA-coated silica sphere array. SEM images of PS nanocylinders using 530 nm silica spheres: (b) straight cylinder with PVA layer and (c) cylinder with blunt tip without PVA layer. (d) SEM image of PS nanocylinders using 320 nm silica spheres. Scale bars are 500 nm.

determined by examining the SEM image of the bottom layer (see Figure S1A in the Supporting Information). Using a sputtering instrument, we then subsequently deposited a thin metal film onto the silica spheres and side wall of the PS nanocylinder. Finally, after the silica spheres were uncapped by sonication in water, O_2 RIE of the PS cores left behind an ordered array of hollow metal nanopillars.

Figure 1A is the side view of a 530 nm silica array coated with PVA over the PS film and silica array. Polymeric double layers could be fabricated by selecting a pair of polymers soluble in different solvents. Degradation of the PS layer was not observed during the PVA coating because the solvent of PVA solution was deionized water, which is a poor solvent for PS. The vacant volume between silica spheres and PS film was filled with PVA. Figure 1B is the cross-sectional SEM image of the PS nanopillar array after RIE of the PVA and PS layers. The PVA layer was a critical factor in controlling the tip shape of the PS nanopillars during the O_2 RIE. As shown in Figure 1B, the PVA layer successfully blocked the under-etching[3a] of the PS surface around the contact point with a silica particle. Consequently, the straight cylindrical PS pillars were formed in the presence of the PVA film. Without the PVA layer, the under-etching of the PS surface forming a blunt cylinder tip was observed, as shown in Figure 1C. The diameter of the PS pillars was adjusted by altering the size of the silica spheres, which could be achieved by either using different size silica in self-assembly or varying the degree of CF_4 RIE to etch the silica particles. Figure 1D shows an array of PS nanopillars with a diameter of 120 nm from an array of 320 nm silica spheres. Although CF_4 RIE is effective for the in situ size reduction of silica spheres, the use of smaller colloids is more appropriate for obtaining higher nanopillar density.

The sidewalls of as-prepared nanopillars were coated with a thin gold film. No special treatments were employed except for low bias (32 W of RF plasma power) and high operating pressure (1×10^{-2} Torr) between cathode and anode plates of our sputtering instrument. In general, the lower bias and higher pressure result in the lower anisotropy of sputtering due to the lower acceleration and shorter mean free path of sputtered elements.[7] Therefore, the shadowing effect due to the silica particle on the nanopillar can be reduced under the present experimental conditions. In addition, the hexagonal array of PS nanopillars affected the side wall coating. The side wall of nanopillars was coated by randomly dispersed (or scattered) metal elements after collision with the neighboring six silica spheres and the bottom layer. After sputtering gold over the PS nanopillars, the consecutive removal of silica spheres by sonication in water and the PS cores by O_2 RIE left behind arrays of hollow gold nanopillars as shown in the SEM images of Figure 2. It is worth pointing out that the hollow nanopillar array can be fabricated directly on diverse substrates, which can be coated with PS film. In addition, the direct formation of template on the substrate enables us to avoid the problem such as inhomogeneous contact between rigid template and substrate, frequently issued during the pattern transfer. The hollow nanopillar arrays shown in images A and B of Figure 2 were fabricated from PS films with different thicknesses of 630 and 280 nm, respectively. To confirm the complete removal of polystyrene inside of the gold nanopillars, we observed some collapsed nanopillars through a high-resolution SEM image. Indeed, no polystyrene residue remained inside the nanopillars (see Figure S1B in the Supporting Information). The PVA filler was used only for the array shown in Figure 2A. In Figure 2A, the hollow gold nanopillars were aligned hexagonally and the tip of the nanopillars was opened widely because of the protection effect of the PVA filler against under-etching. The slight shrinkage of the tip in the inset of Figure 2A was caused by the flexible nature of the thin gold

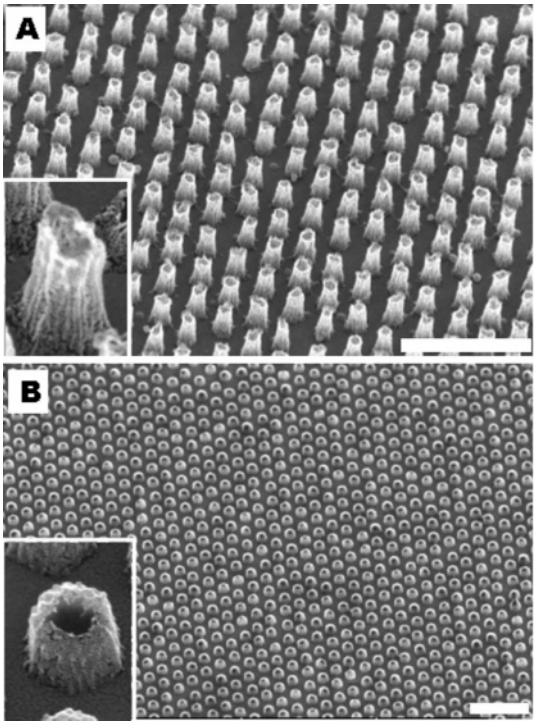

Figure 2. SEM images of hollow gold nanopillar arrays with different height and end-tip shape. (a) Nanopillar array (with a height of 630 nm) from the straight cylinder in Figure 1b. (b) Nanopillar array (with a height of 280 nm) from the cylinder with a blunt tip. Insets are the magnified SEM images of each nanopillar. Scale bars are 2 μm.

(7) Madou, M. J. *Fundamentals of Microfabrication: The Science of Miniaturization*, 2nd ed.; CRC Press: Boca Raton, FL, 2002; pp 77−96.

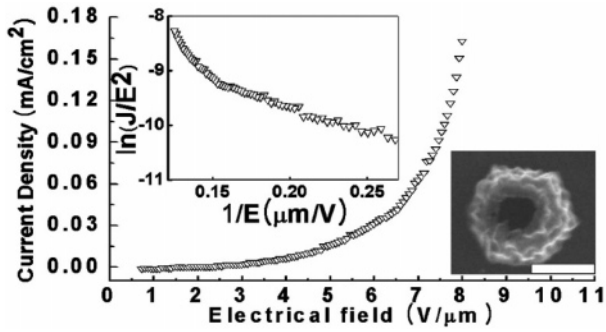

Figure 3. Dependence of the field emission (FE) current density on the applied electric field strength of Mo nanopillar emission tips. Insets are the Fowler−Nordheim plot (left-hand side of the FE curve) and the SEM image of Mo hollow nanopillar (right-hand side of the FE curve), respectively. Scale bar in SEM image is 250 nm.

film, which was about 20 nm thick. Meanwhile, without the PVA filler, the tip end was shrunk appreciably because of the under-etching of the PS layer. In practice, the shell thickness could be controlled from 20 to 50 nm with ease by adjusting the sputtered thickness. The rough surface of the nanopillars shown in the insets of Figure 2 was induced from the surface roughness of the reactive ion-etched polymeric layer[8] and inhomogeneous sputtering of the dispersed metal elements.

As an illustrative purpose, we prepared a molybdenum (Mo) nanopillar array for a field-emission cathode with the same procedure except for the sputtering of Mo instead of gold. The height, inner diameter of the tip end, and tip spacing were about 290, 140, and 530 nm, respectively. Field-emission measurements were conducted in a vacuum chamber under a base pressure of 1×10^{-6} Torr. The electrode spacer with the height of 150 μm was located between a cathode of Mo tube array (1 cm × 1 cm) and an anode of ITO glass. The current−voltage ($I-V$) dependence of the field emission was obtained by applying DC voltage up to 1200 V, and the emission currents were automatically measured. In Figure 3, the field-emission current was plotted as a function of the applied electric field. The turn-on voltage was 4.5 V μm^{-1} at a current density of 10 μA cm^{-2}. As noted, the current density was exponentially increased. The turn-on voltage of the hollow Mo nanopillar array was lower than those of ZnO and MgO nanotubes and comparable with the best result of Mo (2.2 V μm^{-1}) and Mo oxide (3.5 V μm^{-1}) nanowires.[9] The linear trend of the Fowler−Nordheim (FN) plot[10] in the inset verified that the current from the hollow Mo nanopillar array was a field emission. The long-term stability was tested by using a constant dc voltage of 1000 V (equivalent to the electric field of 6.7 V μm^{-1}). In spite of small fluctuations, the current density remained constant for longer than 12 h (see Figure S2 in the Supporting Information). The field enhancement factor, highly related to the top structure of emitter, was calculated to be about 1600 from the slope of the FN plot and the work function of Mo (4.30 V). In accordance with other nanotube emitters, this high enhancement of the electric field was induced from the extremely thin circular tip of the hollow nanopillars.

In summary, ordered hollow nanopillar arrays were fabricated by RIE through colloid arrays self-organized over a polymeric film. Notably, the proposed approach is flexible with respect to variation of morphology and materials. The height of the nanopillars was controlled from 280 to 630 nm by simply adjusting the polymer film thickness. The diameter of the nanopillar was varied from 120 to 350 nm by changing the size of the silica spheres. Furthermore, the shape of the tip end and the shell thickness of the nanopillars could be controlled by coating an additional polymer and varying the sputtering thickness. The fabrication strategy is versatile for preparing the template of polymeric nanopillar arrays onto diverse substrates over large areas and has a wide range of applications. For example, the Mo nanopillar array fabricated here exhibited a low turn-on voltage and can be applied for field emission devices. Also, the present method is able to control the hollow nanotube morphology, which is of practical significance in optical and biotechnology areas.[2a,2b,3b,11]

Acknowledgment. This work was supported by a grant from the Creative Research Initiative Program of the Ministry of Science and Technology. The authors acknowledge partial support from the BK21 Program. We thank Dr. Sora Lee and Yeonju Lee for the field emission measurements.

Supporting Information Available: A detailed description of the experimental procedure (PDF). This material is available free of charge via the Internet at http://pubs.acs.org.

CM060731J

(8) Powell, H. M.; Lannutti, J. J. *Langmuir* **2003**, *19*, 9071.
(9) (a) Shen, X.-P.; Yuan, A.-H.; Hu, Y.-M.; Jiang, Y.; Xu, Z.; Hu, Z. *Nanotechnology* **2005**, *16*, 2039. (b) Wu, M.-S.; Lee, J.-T.; Wang, Y.-Y.; Wan, C.-C. *J. Phys. Chem. B* **2004**, *108*, 16331. (c) Zhou, J.; Xu, N.-S.; Deng, S.-Z.; Chen, J.; She, J.-C.; Wang, Z.-L. *Adv. Mater.* **2003**, *15*, 1835.
(10) Fowler, R. H.; Nordheim, L. W. *Proc. R. Soc. London, Ser. A* **1928**, *119*, 173.
(11) Lamprecht, B.; Schider, G.; Lechner, R. T.; Ditlbacher, H.; Krenn, J. R.; Leitner, A.; Aussenegg, F. R. *Phys. Rev. Lett.* **2000**, *84*, 4721.